BULLETIN OF THE POLISH ACADEMY OF SCIENCES
TECHNICAL SCIENCES, Vol. 66, No. 5, 2018
DOI: 10.24425/125337

Ligament-based spine-segment mechanisms

A. CISZKIEWICZ* and G. MILEWSKI

Institute of Applied Mechanics, Cracow University of Technology, Al. Jana Pawła II, 31-864 Cracow, Poland

Abstract. Nowadays, a growing interest in spine-segment mechanisms for humanoid robots can be observed. The ones currently available are mostly inspired by an intervertebral joint but rarely use its structure and behaviour as input data. The aim of this study was to propose and verify an approach to spine-segment mechanisms synthesis, in which the mechanisms were obtained directly from a ligament system of the intervertebral joint through numerical optimization. The approach consists of two independent optimization procedures performed with genetic algorithm. The first one searches for the optimal structure, while the second estimates its geometrical and stiffness parameters. The mechanisms are rated by their ability to reproduce the static behaviour of the joint in selected aspects. Both procedures use the lumbar L4-L5 intervertebral joint reference data. The approach was tested in two numerical scenarios. It was possible to obtain a mechanism with 7 flexible linear legs that accurately emulated the elastostatic behaviour of the intervertebral joint under moment loads. The results prove that the proposed method is feasible and worth exploring. It may be employed in design of bioinspired joints for use in humanoid robots and can also serve as an initial step in the design of prosthetic and orthotic devices for a human spine.

Key words: intervertebral joint, optimization, parameters estimation, genetic algorithm, elastostatic analysis.

1. Introduction

Due to the recent advancements in manufacturing, electronics and computer science it is now possible to design and produce robots that could relieve people in their daily tasks. These machines are often referred to as humanoids, as they resemble human beings and mimic their motion. In the near future, they may eventually find their use in facilities such as: hospitals, airports, markets and hotels. The resemblance to human beings is owed to their internal structure, often inspired by human body joints. Thus, a growing need for mechanisms that reproduce the behaviour of biological joints can be observed in robotics.

One of the most complex structures in the human body is the spine. It contains 33 vertebrae that form functional spinal units (FSU) also known as intervertebral joints (IJ) – see Fig. 1a. The IJ is a skeletal structure that contains ligaments, a disc and two vertebrae [1, 2]. There are nine ligaments in total: anterior longitudinal ligament (ALL), posterior longitudinal ligament (PLL), supraspinous ligament (SSL), interspinous ligament (ISL), flaval ligament (FL), two intertransverse ligaments (ITL1, ITL2) and two capsular ligaments (FC1, FC2) [3]. Their main function is to transfer tensile loads, while the disc is mostly responsible for compressive loads. Each vertebra also contains geometrical structures called facet joints that are symmetrical and, for the most part, constrain the axial rotation of the vertebrae. As seen in Fig. 1a, the structure of the joint connecting the vertebra is very complex. It works perfectly fine in an organic system, however, it is not feasible as a technical solution.

It is no easy task to represent such a complicated system in a simpler form that is ready for use in humanoid robots. Nevertheless, several research groups have proposed their take on this problem. A popular approach is to represent the spine by a series of 1 to 3 revolute joints [4, 5]. While relatively simple and cost-effective, this solution differs greatly from the spine – both in structure and capabilities. Thus, more complicated parallel mechanisms have been applied. Two different approaches can be distinguished in this area. The first one employs rigid platform mechanisms, as in a hybrid trunk and waist mechanism [6]. The mechanism is a serial composition of two parallel structures. The first one is based on the Stewart platform [7], while the second is an orientation platform with 3 legs. Similar concepts have also been applied in [8, 9]. The second approach uses mechanisms with flexible links. A common solution is to use ball-socket joints complemented by rubber or springs [10, 11], but different approaches are also available: a robotic neck system [12], three-legged parallel mechanism with a flexible rod mirroring the disc [13].

The aforementioned mechanisms often use the IJ as an inspiration but rarely fully explore its structure and responses to load or motion. In this area, the actual models of the joint provide the best results. These models can be divided into two major groups: finite element method (FEM) and multibody system method (MBS) models. The FEM models provide very accurate results, useful when assessing the effort of the joint [3], and can also be used to design artificial discs [14–16]. Nevertheless, due to high numerical complexity, the FEM is usually applied to structures with limited mobility. On the other hand, the MBS is well suited for systems experiencing large displacements, such as a lumbar spine with muscle system [17–19]. As complex viscoelastic sys-

*e-mail: adam.ciszkiewicz@gmail.com

Manuscript submitted 2017-01-22, revised 2017-05-04 and 2017-10-20, initially accepted for publication 2017-11-15, published in October 2018.

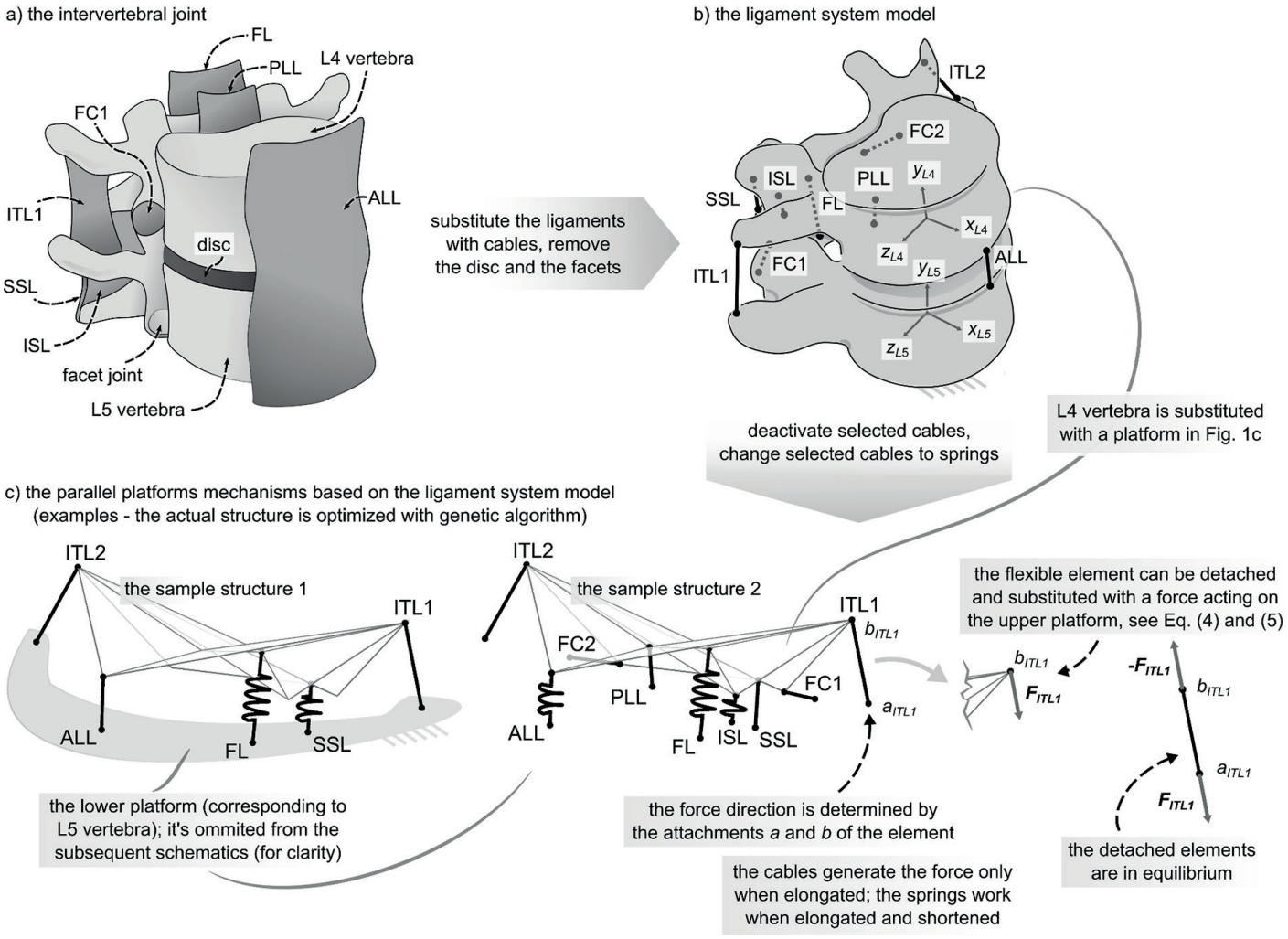

Fig. 1. a) The intervertebral joint, b) the ligament system model with the L4, L5 vertebra for reference (the ligaments are substituted with linear cables), c) the sample parallel platform mechanisms with flexible links, structure and geometry based on the ligament system from Fig. 1b. Coordinate systems: $\{x_{L5}\ y_{L5}\ z_{L5}\}$ – the L5 vertebra reference frame, $\{x_{L4}\ y_{L4}\ z_{L4}\}$ – the L4 vertebra reference frame

tems are difficult to model with this method, the disc is often described with a stiffness matrix [20, 21]. A different approach can be seen in [22], in which the disc is substituted with linear and angular springs. In the mechanism [22] the vertebrae are considered solid and the ligaments are modeled as linear cables. While the disc model presented in [22] is much simpler than the actual structure, the FSU model could be simplified even further. Instead of substituting the disc with an additional set of springs, it may be possible to incorporate it, through optimization, into the already existing set of flexible elements – the ligament system. The optimized ligament system may even have the capacity to incorporate the facet joints, which are difficult to reproduce in a technical solution. This concept could bridge the gap between the simplified spine-segment mechanisms and complex FSU models. To the best of our knowledge, it has never been tested or presented in the literature.

The aim of this study was to propose and verify an approach to spine-segment mechanisms synthesis, in which the mechanisms were obtained from the ligament system of the IJ through numerical optimization. The approach consists of two independent optimization procedures using GA. The first one searches for the optimal structure, while the second estimates its geometrical and stiffness parameters. The mechanisms are rated by their ability to reproduce the angular stiffnesses of the joint. Both procedures use the lumbar L4-L5 FSU reference data.

For the sake of consistency the flexible elements of the mechanism (springs and cables) are referred to as the ligaments (unless the context requires a distinction). The reference frame of the upper (lower) platform is the same as the L4 (L5) vertebra reference frame.

2. Method

2.1. The mechanism structure. As mentioned before, the approach uses the ligament system of the L4-L5 lumbar FSU as an initial structure for the mechanism (see Fig.1b). In the actual joint the ligaments behave similarly to cables [22, 24]. They are aided by the disc and facets and together constitute a complex system that transfers both tensile and compressive loads. As

in our method the disc and the facet joints are omitted, some changes to the ligament system are necessary. We assume that the ligaments may either be cables or springs and some of them may be inactive.

With these assumptions, there are 2^14 possible variations of the proposed 9-ligament structure – checking all of them is not a feasible solution. It is also very difficult to manually adjust the state and the type of the ligaments. Therefore, in this study, the optimal structure problem was addressed with genetic algorithm (GA) [25]. To use GA for this problem, it is necessary to establish the design variables vector. Since the assumed ligament system model contains 9 ligaments (see Fig. 1b) and is symmetric in the sagittal plane $\{x_{L5}\ y_{L5}\}$, 14 binary parameters fully define the structure of the mechanism based on this system. The first 7 determine the type of the ligaments (0 – cable, 1 – spring) while the remaining 7 specify which ligaments are active (0 – inactive; 1 – active). For instance, the first structure (see Fig. 1c) can be described with the following design variables vector: $\boldsymbol{x}_{struct} = [1\ 0\ 1\ 0\ 1\ 1\ 0\ 0\ 0\ 1\ 0\ 1\ 0\ 0]$ – PLL, ISL, FC1/2 are deactivated, while FL, SSL are now springs. The structures based on the ligament system also contain two rigid platforms, which correspond to the vertebrae.

GA has been applied and proven effective in a wide variety of problems ranging from neural network training [26] to power filters allocation [27] and path planning [28]. Its working principle is exemplified in Fig. 2. A solution (mechanism), defined by a design variables vector $\boldsymbol{x}_{struct}$, is referred to as a specimen, while a set of different solutions constitutes a population. The first population is generated randomly, taking into account the boundaries on the design variables and each member of this population is rated with the assumed objective function. Then,

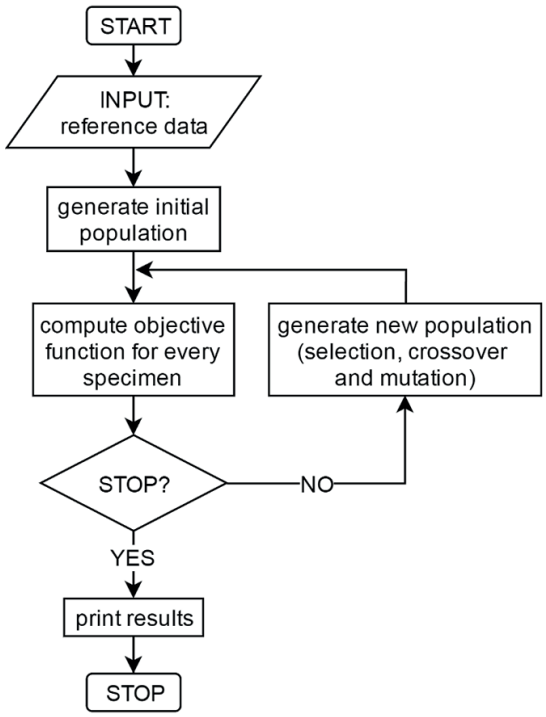

Fig. 2. Genetic algorithm

a children population is obtained from the previous one. This is done in three steps. Firstly, a selection procedure is used to choose parents from the previous population based on their scaled objective function values. Then, crossover-children are created. The process of creating a crossover-child from two parents is defined by the crossover function. Finally, some parents undergo mutation and create mutation-children, which diversify the new population. After this, the children population is rated and the process is repeated. The procedure stops if there is no improvement of solution or the limit of generations has been reached. Based on the implementation, the algorithm can work on binary or real variables – both approaches are utilized in this study.

The parameters of GA used in the structure optimization are summarized in Table 1. In this case the search was not constrained. It is worth noting that the results are highly dependent on the initial geometric and material parameters of the assumed ligament system. We tested different combinations and the best structure was obtained using the ligaments with the geometry obtained from a 3D spine scan and the stiffness coefficients of 250.00 N/mm.

Table 1
The parameters of GA (MATLAB's implementation).

type	binary coded – structure optimization; real coded – parameters estimation
objective function scaling	rank-based
selection	stochastic universal sampling
mutation	adaptive feasible
crossover	scattered
crossover (elite) fraction	0.82 (0.05)
population size	60
generations	500

2.2. The objective function. The purpose of the presented approach is to obtain simple mechanisms with static load responses comparable to that of the FSU. Therefore, the problem requires a measure of the mechanism quality. In this study, the models were rated by comparing their angular displacements, under static moment loads, to that of a reference (here: a verified model of the L4/L5 FSU). The moment loads were applied in 33 variants (11 for each: flexion, lateral bending and axial rotation). This choice corresponds to the most common experimental studies of the IJ. The results of such experiments are usually presented as a set of load-displacement curves [29] – often, only moment – angular displacement. In order to measure the quality of the mechanism three indicators are necessary:

$$diff_x = \frac{\sum_{i=1}^{11} \left| \Delta x(\mathrm{M}_{xi}) - \Delta x_{ref}(\mathrm{M}_{xi}) \right|}{\max(\Delta x_{ref}) - \min(\Delta x_{ref})}, \tag{1}$$

where: $x \in \{\alpha$ – flexion, β – lateral bending, γ – axial rotation$\}$, thus: $diff_\alpha$ – the flexion displacement indicator; $\Delta\alpha$ – the angular displacement obtained from the mechanism at flexion moment

of value $M_{\alpha i} = 0..10$ Nm ($\Delta M_{\alpha i} =$ Nm), $\Delta\alpha_{ref}$ – the reference angular displacement measured on the actual joint or obtained from a verified joint model at flexion moment $M_{\alpha i} = 0..10$ Nm ($\Delta M_{\alpha i} = 1$ Nm). The remaining quantities can be defined in a similar way.

The objective function, that computes the difference between the displacements of the mechanism and that of the actual joint, under three, different load cases, can be defined as follows:

$$h(\boldsymbol{x}) = w_1 diff_\alpha + w_2 diff_\beta + w_3 diff_\gamma + w_4 not\_passed, \quad (2)$$

where: $h()$ – the objective function, w_i – the weight i (here: $w_i = 1$ [$i = 1..3$], $w_4 = 2$), *not_passed* – the number of loading conditions for which the solver doesn't converge to a solution in under 200 iterations (for a mechanism with a good structure, operating far from singular locations, the solution is likely to be obtained in under 75 iterations).

2.3. The elastostatic model of the mechanism. The mechanism model, used to compute (1), is based on the equilibrium equations. This method has also been applied in [22]. The equation set that defines the equilibrium of the upper platform is as follows:

$$\begin{cases} \sum_{i=1}^{n} \boldsymbol{F}_{ci} + \sum_{j=1}^{m} \boldsymbol{F}_{sj} + \boldsymbol{F}_{ext} = 0 \\ \sum_{i=1}^{n} \boldsymbol{M}_{ci} + \sum_{j=1}^{m} \boldsymbol{M}_{sj} + \boldsymbol{M}_{ext} = 0, \end{cases} \quad (3)$$

where: $\boldsymbol{F}_s(\boldsymbol{M}_s)$ – the forces (moments) generated by the linear springs, $\boldsymbol{F}_{ext}(\boldsymbol{M}_c)$ – the forces (the moments) generated by the linear cables, $\boldsymbol{F}_{ext}(\boldsymbol{M}_{ext})$ – the external force (moment) acting on the upper platform, $n(m)$ – the number of the springs (cables).

The force and moment corresponding to a linear spring element s are computed in the following way:

$$\begin{aligned} F_s &= -k_s \Delta l_s, \quad \boldsymbol{F}_s^o = \frac{\boldsymbol{b}_s - \boldsymbol{a}_s}{\|\boldsymbol{b}_s - \boldsymbol{a}_s\|}, \\ \boldsymbol{F}_s &= \boldsymbol{F}_s^o F_s, \quad \boldsymbol{M}_s = \boldsymbol{b}_s \times \boldsymbol{F}_s, \end{aligned} \quad (4)$$

where: $\boldsymbol{F}_s(\boldsymbol{M}_s)$ – the force (moment) generated by the linear spring, k_s – the stiffness parameter for the spring element, Δl_s – the change of the spring element length, $\boldsymbol{a}_s(\boldsymbol{b}_s)$ – the position vector of the spring element attachment to the lower (upper) platform.

The force and moment corresponding to a linear cable element c are obtained in a similar way, only the magnitude of the force is computed differently:

$$F_c = \begin{cases} -k_c \Delta l_c, & \text{for} \quad \Delta l_c > 0 \\ 0, & \text{for} \quad \Delta l_c \le 0, \end{cases} \quad (5)$$

where: k_c – the stiffness parameter for the cable element, Δl_c – the change of the cable element length.

The set of 6 nonlinear equations (3) can be solved with numerical equation solvers, such as the ones provided in MATLAB. The 6 unknown variables in (3) have the following physical meaning: the first 3 of them form the translation vector $\boldsymbol{p}_{L4L5}$ between the origins of the upper and lower platform reference frame (coincident with L4 and L5 vertebra reference frame):

$$\boldsymbol{p}_{L4L5} = \begin{bmatrix} p_x & p_y & p_z \end{bmatrix}^T, \quad (6)$$

while the remaining 3 are the angular coordinates α, β, γ that correspond subsequently to the flexion, lateral bending and axial rotation of the upper platform with regard to the lower platform. These determine the rotation matrix between the platforms:

$$\boldsymbol{R}_{L4L5} = \begin{bmatrix} c\alpha c\gamma + s\alpha s\beta s\gamma & -s\alpha c\gamma + c\alpha s\beta s\gamma & -c\beta s\gamma \\ s\alpha c\beta & c\alpha c\beta & s\beta \\ c\alpha s\gamma - s\alpha s\beta c\gamma & -s\alpha s\gamma - c\alpha s\beta c\gamma & c\beta c\gamma \end{bmatrix}, \quad (7)$$

where: $\boldsymbol{R}_{L4L5}$ – the rotation matrix from the upper to the lower platform reference frame, $s\alpha = \sin\alpha$, $c\alpha = \cos\alpha$. The sequence of rotations was assumed after [24, 30].

The flexion α is an angular coordinate about the z_{L4} axis of the L4 vertebra reference frame (z_{L4} is orthogonal to the sagittal plane of the moving vertebra), the internal rotation γ occurs about the y_{L5} axis of the L5 vertebra reference frame (y_{L5} is orthogonal to the transverse plane of the base vertebra), while the abduction β is an angular coordinate about a floating axis that is perpendicular to the z_{L4} and the y_{L5} [24].

2.4. The parameters estimation. In order to fully incorporate the behaviour of the disc and facet joints into the ligament system with the optimized structure (see section 2.1), the parameters estimation is necessary. Since the structure contains flexible elements, both the attachments to the platforms and stiffness coefficients should be estimated.

In this study, two different approaches to the free length of the springs and cables were tested. For the first one, it was assumed that the free length was determined by the initial geometry of the joint, obtained from a 3D scan. Hence, given an initial location of the L4 vertebra with regard to the L5 vertebra, the free length could be computed. In this case, the design variables vector for parameters estimation $\boldsymbol{x}_{par\_est}$ contained 32 real-valued parameters (the inactive ligaments weren't further optimized). For the second one, the free lengths were estimated with the other parameters – the design variables vector $\boldsymbol{x}_{par\_est}$ contained 38 parameters. The latter approach resulted in a more time-consuming numerical procedure. However, it was more general and returned better results.

The estimation of geometrical and stiffness parameters was performed using GA. The algorithm was setup as in Table 1 and the objective function for the parameters estimation was defined as in structure optimization (see (2). The bounds for the design variables representing the ligament attachments were based on the actual FSU geometry. For instance the lower LB_{aix}

Table 2
The input data set

Non–symmetric ligaments					
	$\boldsymbol{a}_{ALL}$	$\boldsymbol{a}_{PLL}$	$\boldsymbol{a}_{SSL}$	$\boldsymbol{a}_{ISL}$	$\boldsymbol{a}_{FL}$
x [mm]	20.71	–17.20	–55.29	–46.63	–34.97
y [mm]	22.14	22.83	6.10	9.06	7.95
z [mm]	0.00	0.00	0.00	0.00	0.00
	$\boldsymbol{b}^{L4}_{ALL}$	$\boldsymbol{b}^{L4}_{PLL}$	$\boldsymbol{b}^{L4}_{SSL}$	$\boldsymbol{b}^{L4}_{ISL}$	$\boldsymbol{b}^{L4}_{FL}$
x [mm]	19.41	–16.78	–58.65	–50.65	–39.28
y [mm]	–3.50	–0.73	–11.10	–13.73	–2.72
z [mm]	0.00	0.00	0.00	0.00	0.00
k [N/mm]	250.00	167.00	56.00	100.00	43.00
act [–]	1	1	1	1	1
beh [–]	0	0	0	0	0

Symmetric ligaments				
	$\boldsymbol{a}_{ITL1}$	$\boldsymbol{a}_{ITL2}$	$\boldsymbol{a}_{FC1}$	$\boldsymbol{a}_{FC2}$
x [mm]	–26.20	–26.20	–32.04	–32.04
y [mm]	24.40	24.40	21.65	21.65
z [mm]	49.67	–49.67	31.76	–31.76
	$\boldsymbol{b}^{L4}_{ITL1}$	$\boldsymbol{b}^{L4}_{ITL2}$	$\boldsymbol{b}^{L4}_{FC1}$	$\boldsymbol{b}^{L4}_{FC2}$
x [mm]	–30.19	–30.19	–37.40	–37.40
y [mm]	10.01	10.01	–8.96	–8.96
z [mm]	42.16	–42.16	21.31	–21.31
k [N/mm]	50.00	50.00	62.50	62.50
act [–]	1	1	1	1
beh [–]	0	0	0	0

and upper UB_{aix} bound on the x-coordinate of the i-th ligament's attachment a (see Table 2) was obtained as follows:

$$\begin{aligned} LB_{aix} &= a_{ix} - 15.00 \text{ mm}, \\ UB_{aix} &= a_{ix} + 15.00 \text{ mm}. \end{aligned} \tag{8}$$

The bounds on the stiffness coefficients were computed using the material properties of the joint (see Table 2):

$$\begin{aligned} LB_{ki} &= \min(k_{ALL}, k_{PLL}, \ldots, k_{FL}), \\ UB_{ki} &= \max(k_{ALL}, k_{PLL}, \ldots, k_{FL}). \end{aligned} \tag{9}$$

Since the actual free lengths of the ligaments are difficult to obtain, their bounds were arbitrarily set to:

$$LB_{li} = 5.00 \text{ mm}, \quad UB_{li} = 100.00 \text{ mm}. \tag{10}$$

2.5. The input data set. The input data set for the procedure is presented in Table 2. It contains:

- $\boldsymbol{a}_i$ – the position vector of the ligament i attachment to the L5 vertebra in the L5 vertebra reference frame,
- $\boldsymbol{b}_i^{L4}$ – the position vector of the ligament i attachment to the L4 vertebra in the L4 vertebra reference frame,
- k_i – the stiffness of the ligament i, obtained by linearizing the experimental force-displacement curves presented in [23],
- beh_i – the type of the ligament i (0 – cable, 1 – spring),
- act_i – the state of the ligament i (0 – inactive, 1 – active),

where $i \in \{\text{ALL, PLL, SSL, ISL, FL, ITL1, ITL2, FC1, FC2}\}$. The reference data, required for the parameters estimation, was assumed after [3].

The procedure also requires the initial location of the L4 vertebra with regard to the L5 vertebra reference frame (obtained from the 3D scan), which is described by the vector $\boldsymbol{q}_0 = [\alpha_0 \ \beta_0 \ \gamma_0 \ p_{x0} \ p_{y0} \ p_{z0}]^{\mathrm{T}}$. Here: $\boldsymbol{q}_0 = [7.57 \text{ deg } 0.00 \text{ deg } 0.00 \text{ deg } -0.17 \text{ mm } 35.22 \text{ mm } 0.00 \text{ mm}]^{\mathrm{T}}$.

The initial geometry of the ligament system was extracted from lumbar L4-L5 FSU scan by BodyParts3D (© The Database Center for Life Science licensed under CC Attribution-Share Alike 2.1 Japan). The L5 vertebra was assumed to be the basis of the structure.

3. Results

The presented approach was used to obtain a simple spine-segment mechanism. The structure optimization and parameters estimation were performed using the input data set presented paragraph 2.5. The obtained mechanism is visualized in Fig. 3. Since 2 capsular ligaments (FC) have been excluded from the ligament system through structure optimization, the mechanism consists of only 7 flexible elements – 3 linear springs and 4 linear cables. The spring-ligaments give the model the ability to transfer varied moment loads along all three axes of the L5 reference frame. It is worth mentioning that the geometry of the system still resembles that of the L4-L5 FSU, on which it is based. The results are summarized in Table 3, while

Table 3
Simulation results: *MaxDiff* (*MeanDiff*) – maximum (mean) relative difference between results obtained from the proposed mechanism and reference data, *RefRange* – the range of the angular displacements obtained from the reference data

Free lengths: the first approach	**α**	**β**	**γ**
MaxDiff [%]	7.95	25.47	22.80
MeanDiff [%]	2.32	11.35	9.50
RefRange [deg]	6.85	6.14	2.50

Free lengths: the second approach	**α**	**β**	**γ**
MaxDiff [%]	8.14	10.76	8.78
MeanDiff [%]	5.40	5.74	2.06
RefRange [deg]	6.85	6.14	2.50

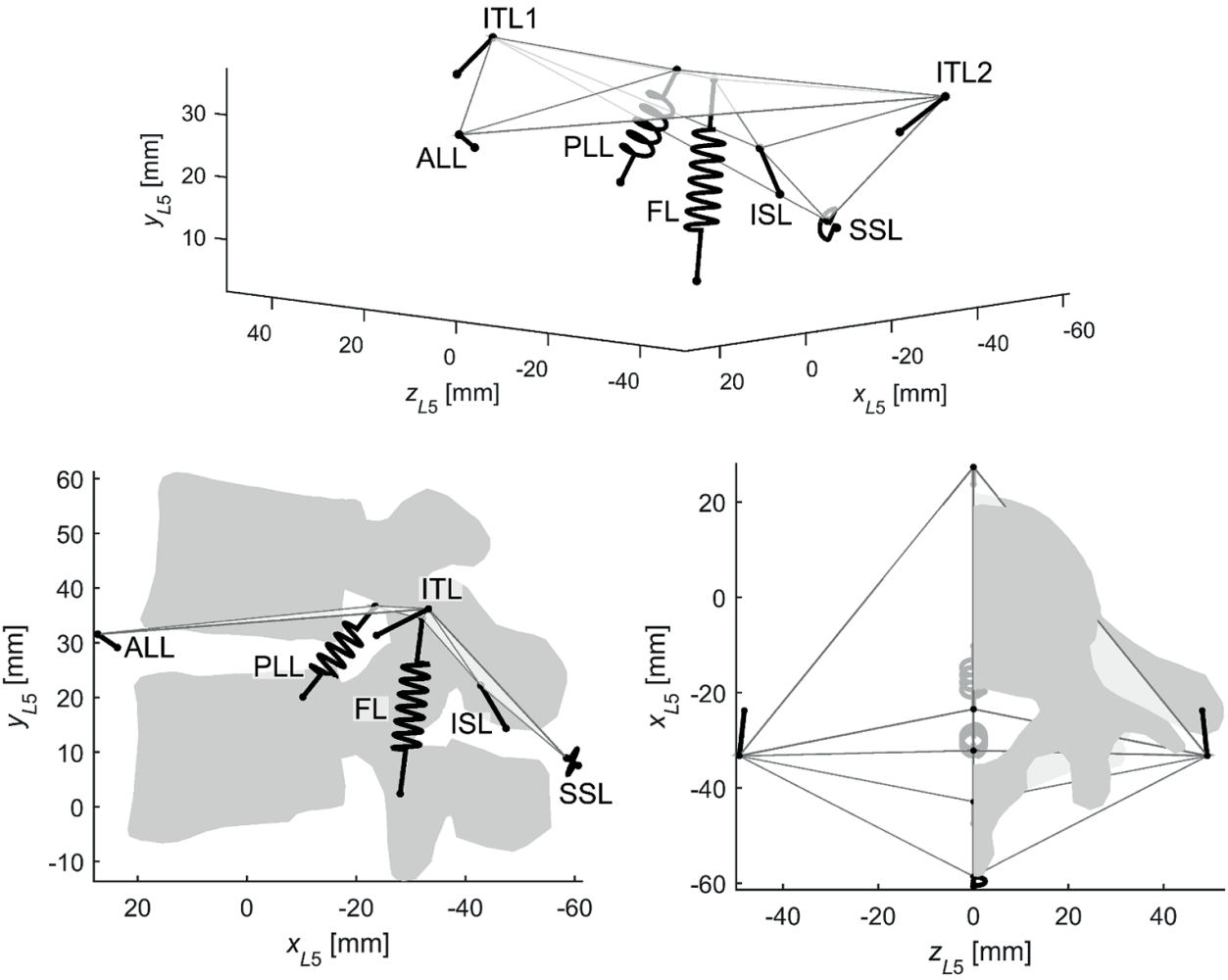

Fig. 3. The obtained parallel platform mechanism with flexible links in 3 different views with the L4, L5 vertebra for reference. For clarity the lower platform of the mechanism is omitted from the image. Coordinate systems: $\{x_{L5}\ y_{L5}\ z_{L5}\}$ – the L5 vertebra reference frame

Fig. 4 contains the load-displacement curves obtained from the mechanism and reference data.

It is notable that with the free lengths estimated, the obtained results are significantly better. This is especially evident when considering the maximum difference between the mechanism and reference. In this case, the mean difference is between 2.06% and 5.74%. This is a good result, which signifies that a simplified mechanism can be derived directly from the ligament system of the FSU.

4. Discussion

As aforementioned, the mechanisms [12, 13, 31] retain general FSU features, however, cannot accurately reproduce the complex static behaviour of the human IJ. On the other hand, the available models of the IJ are often too complex to be used as a technical solution. The mechanism obtained using the presented approach is very close to the geometry and responses of an actual lumbar spine FSU (L4-L5). In some applications, this human-like geometry and response to static loads may be desirable. The obtained structure contains only 7 linear flexible elements and 2 rigid platforms – simple when compared to the IJ and its models. Furthermore, the behaviour of the disc and facet joints was successfully incorporated into the structure of the mechanism through numerical optimization. The modified ligament system doesn't require any additional structures to transfer the typical loads for the FSU. These significant simplifications make it a potentially feasible technical solution.

The performance of the mechanism with the estimated free lengths is very good as the maximum difference between the reference data and the mechanism response is at 8% for the flexion and at 11% and 9% for the lateral bending and axial rotation respectively. The mean difference can be as low as 2% for the axial rotation and less than 6% for the flexion and lateral bending. When considering that the differences between the static tests of the IJ are significant (up to at 2.5 deg flexion at 10 Nm moment [32, 33]), the obtained results are more than

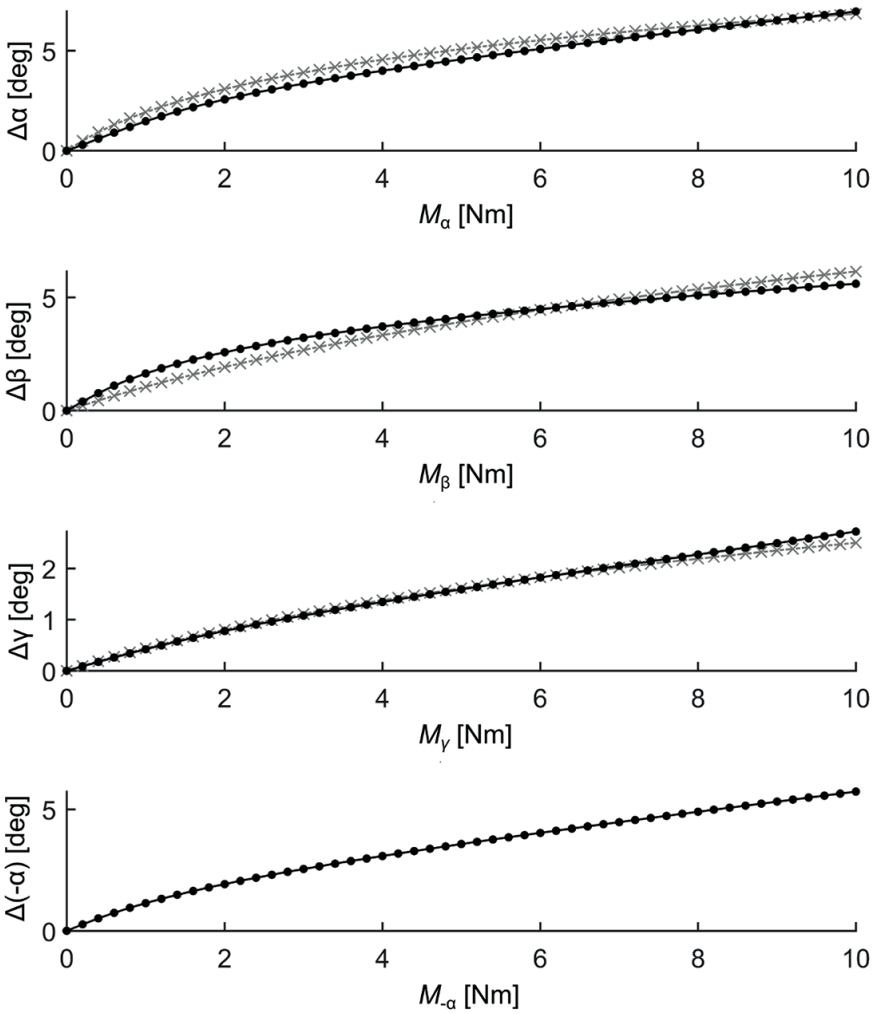

Fig. 4. Simulation results (free lengths: the second approach): graphs of moment loads acting on the system and the angular displacements they cause (“.” marker – the data obtained from the mechanism, “x” marker – the reference data), where: α – the flexion, β – the lateral bending, γ – the axial rotation, –α – the extension

satisfactory. Even though the extension displacement was not included in the optimization, it corresponds well with the reference data [3]. The obtained mechanism closely reproduces the angular stiffnesses of the IJ.

5. Conclusion

In this study, an automated approach to spine-segment mechanisms synthesis was presented. The procedure consists of a purely numerical search for an optimal structure and its parameters under a given criterion (here: the response to static loads). The search is constrained by the geometry and material properties of the IJ ligament system.

The approach was used to obtain a simple spatial mechanism capable of reproducing the static behaviour of the lumbar IJ. It was shown that the obtained system mimicked the angular displacements of the FSU under moment loads, while retaining a simple structure and geometry – all of its elements were either linear springs or linear cables. The approach can be used as a first step in design of spine-modules for humanoid robots or orthotics for the lumbar spine.

The presented method can now be extended to a simultaneous search for the optimal structure and its parameters. This would alleviate the problem of defining the initial parameters for the structure optimization. Future work will also be focused on adding collision and strength models to the procedure. This, in turn, will open up new research problems concerning prototyping, experimental testing of the obtained structures and methods for introducing them into humanoid robots.

References

[1] J.F. Behrsin and C.A. Briggs, “Ligaments of the lumbar spine: a review.”, *Surg. Radiol. Anat.* 10 (3), 211–219 (1988).
[2] P. Sarathi Banerjee, “Morphological and Kinematic Aspects of Human Spine – As Design Inputs for Developing Spinal Implants”, *J. Spine*. 2 (4), 2–5 (2013).

[3] B. Weisse, et al., "Determination of the translational and rotational stiffnesses of an L4-L5 functional spinal unit using a specimen-specific finite element model", *J. Mech. Behav. Biomed. Mater.* 13, 45–61 (2012).
[4] O. Yu, et al., "Development of a New Humanoid Robot WABIAN-2*", *Proc. 2006 IEEE Int. Conf. Robotics and Automation, ICRA 2006,* 76–81 (2006).
[5] N.G. Tsagarakis, et al., "Lower body design of the "iCub" a human-baby like crawling robot", *Proc. 2006 6th IEEE-RAS Int. Conf. Humanoid Robot. HUMANOIDS*, 450–455 (2006).
[6] C. Liang and M. Ceccarelli, "Design and simulation of a waist-trunk system for a humanoid robot", *Mech. Mach. Theory* 53, 50–65 (2012).
[7] D. Stewart, "A platform with six degrees of freedom", *Proc. IMechE*. 180(1), 371–385 (1965).
[8] R.N.E. Nava, G. Carbone, and M. Ceccarelli, "CaPaMan2bis as trunk module in CALUMA (CAssino low-cost hUMAnoid robot)", *Proc. 2006 IEEE Conf. Robot. Autom. Mechatronics*, (2006).
[9] A. Ciszkiewicz and G. Milewski, "A novel kinematic model for a functional spinal unit and a lumbar spine", in *Acta Bioeng. Biomech.* 18(1), 87–95 (2016).
[10] I. Mizuuchi, R. Tajima, T. Yoshikai, and D. Sato, "The Design and Control of the Flexible Spine of a Fully Tendon-Driven Humanoid «Kenta»", *Proc. 2002 IEEE/RSJ Int. Conf. Int. Robots Systems,* 2527–2532 (2002).
[11] F. Guenter, L. Roos, A. Guignard, and A.G. Billard, "Design of a biomimetic upper body for the humanoid robot Robota", *Proc. 2005 5th IEEE-RAS Int. Conf. Humanoid Robot.,* 56–61 (2005).
[12] B. Gao, et al., "Inverse kinematics and workspace analysis of a cable-driven parallel robot with a spring spine", *Mech. Mach. Theory* 76, 56–69 (2014).
[13] C. Cibert and V. Hugel, "Compliant intervertebral mechanism for humanoid backbone: Kinematic modeling and optimization", *Mech. Mach. Theory* 66, 32–55 (2013).
[14] P. Borkowski, et al., "Finite element analysis of an elastomeric artificial disc in lumbar spine", in *Acta Bioeng. Biomech.* 14(1), 59–66 (2012).
[15] M. Pawlikowski, K. Skalski, and T. Sowiński, "Hyper-elastic modelling of intervertebral disc polyurethane implant", in *Acta Bioeng. Biomech.* 15(2), 43–50 (2013).
[16] F. García Vacas, F. Ezquerro Juanco, A. Pérez De La Blanca, M. Prado Novoa, and S. Postigo Pozo, "The flexion-extension response of a novel lumbar intervertebral disc prosthesis: A finite element study", *Mech. Mach. Theory* 73, 273–281 (2014).
[17] M. Christophy, N.A.F. Senan, J.C. Lotz, and O.M. O'Reilly, "A Musculoskeletal model for the lumbar spine", *Biomech. Model. Mechanobiol.* 11(1–2), 19–34 (2012).
[18] M. de Zee, L. Hansen, C. Wong, J. Rasmussen, and E.B. Simonsen, "A generic detailed rigid-body lumbar spine model", *J. Biomech.* 40(6), 1219–1227 (2007).
[19] T.K. Rupp, W. Ehlers, N. Karajan, M. Günther, and S. Schmitt, "A forward dynamics simulation of human lumbar spine flexion predicting the load sharing of intervertebral discs, ligaments, and muscles.", *Biomech. Model. Mechanobiol.* 14(15), 1081–1105 (2015).
[20] G. Desroches, C.E. Aubin, D.J. Sucato, and C.H. Rivard, "Simulation of an anterior spine instrumentation in adolescent idiopathic scoliosis using a flexible multi-body model", *Med. Biol. Eng. Comput.* 45(8), 759–768 (2007).
[21] M. Christophy, M. Curtin, N.A. Faruk Senan, J.C. Lotz, and O.M. O'Reilly, "On the modeling of the intervertebral joint in multibody models for the spine", *Multibody Syst. Dyn.* 30(4), 413–432 (2013).
[22] M.R. Gudavalli and J.J. Triano, "An analytical model of lumbar motion segment in flexion", *J. Manipulative Physiol. Ther.* 22(4), 201–208 (1999).
[23] T.H. Pingel, "Beitrag zur Herleitung und numerischen Realisierungeines mathematischen Modells der menschlichen Wirbelsaüle", *Communications from Institute of Mechanics* 77, (1991) [in German].
[24] N. Sancisi and V. Parenti-Castelli, "A new approach for the dynamic modelling of the human knee", PhD thesis, University of Bologna, Bologna, 2008.
[25] D.E. Goldberg, *Genetic algorithms in Search, Optimization and Machine Learning*, Addison-Wesley Longman Publishing Co., Inc., Boston, 1989.
[26] A. Blanco, M. Delgado, and M.C. Pegalajar, "A real-coded genetic algorithm for training recurrent neural networks.", *Neural Netw.* 14(1), 93–105 (2001).
[27] M. Maciazek and M. Pasko, "Optimum allocation of active power filters in large supply systems", *Bull. Pol. Ac.: Tech.* 64(1), 37–44 (2016).
[28] P. Cai, Y. Cai, I. Chandrasekaran, and J. Zheng, "Parallel genetic algorithm based automatic path planning for crane lifting in complex environments", *Autom. Constr.* 62, 133–147 (2016).
[29] I. Yamamoto, M.M. Panjabi, T. Crisco, and T. Oxland, "Three-dimensional movements of the whole lumbar spine and lumbosacral joint.", *Spine* 14(11), 1256–1260 (1989).
[30] E.S. Grood and W.J. Suntay, "A joint coordinate system for the clinical description of three-dimensional motions: application to the knee.", *J. Biomech. Eng.* 105(2), 136–144 (1983).
[31] Y. Wei, Y. Chen, Y. Yang, and Y. Li, "A soft robotic spine with tunable stiffness based on integrated ball joint and particle jamming", *Mechatronics* 33, 84–92 (2016).
[32] A.F. Tencer, "Some Static Mechanical Properties of the Lumbar Intervertebral Joint, Intact and Injured", *J. Biomech. Eng.* 104(3), 193–201 (1982).
[33] M.M. Panjabi, T.R. Oxland, I. Yamamoto, and J.J. Crisco, "Mechanical behavior of the human lumbar and lumbosacral spine as shown by three-dimensional load-displacement curves.", *J. Bone Joint Surg. Am.* 76(3), 413–424 (1994).